하이브리드 MOM/UTD 방법을 이용한 주름진 표면파 안테나의 해석

Analysis of Corrugated Surface Wave Antenna Using Hybrid MOM/UTD Method

김중표 · 이창원 · 손 현

Joong-Pyo Kim · Chang-Won Lee · Hyon Son

요 약

평행평판 도파관으로부터 급전되어지는 주름진 도체판을 가지는 표면파 안테나의 해석이 고려되어진다. 해석의 단순함을 위해 원래의 문제를 3개의 영역, 즉 단락된 평행평판 도파관 내부 구조(내부 영역 1)와 주름진 격자 내부의 구조(내부 영역 2)와 도체 쇄기의 구조(외부 영역)로 나누기 위해 등가원리가 도입된다. End-fire 복사를 하는 주름진 표면파 안테나를 해석하기 위하여 하이브리드 MOM/UTD 방법이 적용되어진다. 수치해석 결과들은 이전의 실험 결과들과 매우 잘 일치하며, 이전의 단순 등가전류 접근의 결과들과 비교할 때 더 나은 결과들이 얻어진다. 또한 효과적인 end-fire 주름진 표면파 안테나 설계를 위한 인자들을 얻을 수 있다.

Abstract

The analysis of a surface wave antenna with the corrugated ground plane fed by a parallel-plate waveguide is considered. An equivalent theorem is employed to subdivide the original problem into three regions for the simple analysis: one concerning the geometry inside the shorted parallel-plate(Internal region 1), one concerning the geometry of the corrugation(Internal region 2), and one concerning the geometry of the conducting wedge(External region). The hybrid method of moment(MOM)/uniform geometrical theory of diffraction(UTD) method is applied to analyze a corrugated surface wave antenna with the end-fire radiation. Our numerical results are very well matched with those of the previous experiment, better results are obtained when compared with those of the previous simple equivalent current approach. Also, we can obtain the parameters to design an effective end-fire corrugated surface wave antenna.

I. Introduction

A surface wave which comprise the corrugations running transverse to the direction of propagation can support surface wave instead of the dielectric-clad ground plane often called to as a surface wave structure. The theory of a surface wave

경북대학교 전자공학과(Department of Electronics, Kyungpook National University)

· 논 문 번 호 : 981118-116

· 수정완료일자 : 1999년 2월 1일

antenna with a corrugated ground plane has been supplied by many investigations[1]~[3]. A surface wave antenna with the corrugated ground plane fed by a parallel-plate waveguide was analyzed and compared with the experiment result[4]. However, in this analysis, very simplified equivalent magnetic currents on the parallel-plate waveguide aperture and the corrugation apertures were used, thus the result of the analysis are not matched with those of the experiment.

Therefore, in this paper, we proposed a new method to obtain better results than the previous approximate method. The analysis of corrugated surface wave antenna is performed by employing the equivalence theorem[5],[6] and reducing the original problem to three simpler cofigurations: one concerning the geometry inside the shorted parallel-plate(Internal region 1), one concerning the geometry of the corrugation(Internal region 2), and one concerning the geometry of the perfectly conducting wedge(External region). The Green's function of the external region is obtained by using UTD[7],[8], those of the in- ternal regions are analytically obtained by using the mode functions in each region. By applying the boundary condition and using method of moment, the fields in each region are calculated. The solution technique presented in this paper will be referred to as a hybrid MOM/UTD method here. Our method gives much better results when comparing with the previous method. The influences of the change of the propagation constant β/k_0 and height of parallel-plate waveguide on the radiation pattern are investigated to obtain the parameters to design a practical end-fire corrugated surface antenna.

Ⅱ. Formulation

The geometry of the problem is sketched in Fig. 1, where a perfectly conducting ground plane with the surface loaded by a finite set of rectangular corrugations is shown. The geometrical and electrical characteristics of the structure are uniform along z-axis. The feed is a parallel-plate with the upper plate opened toward +x direction. It is assumed that a TEM field is incident upon the slot aperture, whose electric and magnetic fields are given by

$$\underline{E}^{inc} = \frac{V}{h} e^{-jkx} \hat{y}$$
$$\underline{H}^{inc} = \frac{V}{\eta h} e^{-jkx} \hat{z} \qquad (1)$$

in which V is the potential difference across the plates, h is the height of the guide, $\eta = \sqrt{\mu/\varepsilon}$, $k = \omega\sqrt{\mu\varepsilon}$, and $\varepsilon = \varepsilon_0\varepsilon_r$. If the y-component of electric field in the aperture of the parallel-plate waveguide and the x-component of electric field in the aperture of the corrugations were known, one would have all information needed to compute the fields in all regions. Hence, we employ the equivalence principle to separate the problem into three simpler configurations. The aperture surfaces are metallized and the equivalent surface currents $\pm\underline{M}_z^p$ and $\pm\underline{M}_z^{c,l}$ are placed at the

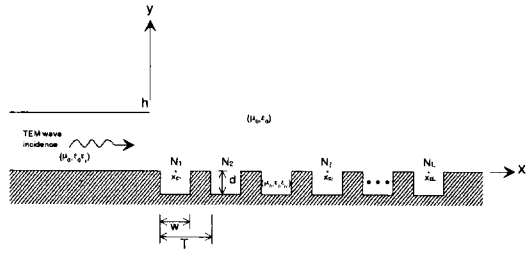

Fig. 1. Geometry of the problem.

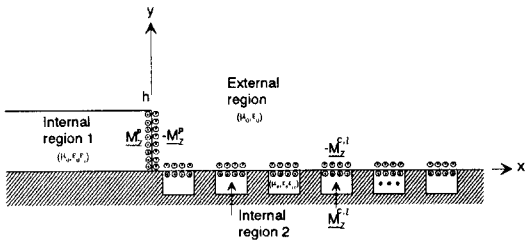

Fig. 2. Decomposition of the original problem into three regions.

both sides of the surfaces, respectively. The equivalent structure is sketched in Fig. 2.

Based on the model of equivalence, the total magnetic field inside the shorted guide is

$$H_z = H_z^{sc} + H_z^{p} \tag{2}$$

where the so-called interior short circuit magnetic field is

$$H_z^{sc} = \frac{V}{\eta h}(e^{-jkx} + e^{+jkx}) = 2\frac{V}{\eta h}\cos(kx), \tag{3}$$

and the magnetic field in the guide due to the magnetic current M_z^p of aperture of parallel-plate and its image is

$$H_z^p = -j\frac{k_0}{\eta_0}\varepsilon_r\int_0^h M_z^p(y')G^p(x,y;0,y')dy'. \tag{4}$$

where $\eta_0 = \sqrt{\mu_0/\varepsilon_0}$, $k_0 = \omega\sqrt{\mu_0\varepsilon_0}$, and the Green's function $G^p(x,y;0,y')$ is

$$G^p(x,y;0,y') = \sum_{q=0}^{\infty}\frac{\alpha_q}{hjk_q}\cos(\frac{q\pi}{h}y') \cdot \cos(\frac{q\pi}{h}y)e^{jk_q x} \tag{5}$$

in which $k_q = \sqrt{k^2 - (q\pi/h)^2}$, α_q is defined by

$$\alpha_q = \begin{cases} 1, & p = 0. \\ 2, & p \neq 0. \end{cases} \tag{6}$$

The magnetic field inside the l-th cavity due to the $M_z^{c,l}$ is

$$H_z^{c,l} = -j\frac{k_0}{\eta_0}\varepsilon_{rc}\int_{C_l} M_z^{c,l}(x') \cdot G^{c,l}(x,y;x',0)dx. \tag{7}$$

where C_l is the l-th cavity aperture path, ε_{rc} is the relative dielectric constant of the cavity region and the Green's function $G^{c,l}(x,y;x',0)$ is derived as

$$G^{c,l}(x,y,;x',0) = \sum_{q=0}^{\infty}\frac{\alpha_q}{wk_q^c}\cos\frac{q\pi}{w} \cdot (x' - x_{cl} - \frac{w}{2})\cos\frac{q\pi}{h}(x - x_{cl} - \frac{w}{2}) \cdot \frac{\cos k_q^c(y+d)}{\sin k_q^c d} \tag{8}$$

where, $k_q^c = \sqrt{k_c^2 - (q\pi/h)^2}$, x_{cl} is the center position of the l-th cavity, w is the corrugation width.

The magnetic field of the external region is the field radiated by the equivalent magnetic current $M_z^{c,l}$ in the presence of the metallic wedge. H_z^{ext} can be represented as

$$H_z^{ext} = \frac{k_0}{4\eta_0}\int_0^h M_z^p(y')G^{ext}(x,y;0,y')dy' + \frac{k_0}{4\eta_0}\sum_{l=1}^{L}\int_{C_l} M_z^{c,l}(x')G^{ext}(x,y;x',0)dx' \tag{9}$$

where G^{ext} is expressed as

$$G^{ext}(x,y;x',y') = G^{direct}(x,y;x',y') + G^{diff}(x,y;x',y'). \tag{10}$$

where $G^{direct}(x,y;x',y')$ an $G^{diff}(x,y;x',y')$ consist of the geometrical optics(GO) terms and the wedge diffracted terms, respectively. The region separation of geometrical structure to obtain

the external Green's function is shown in Fig. 3, and the wedge diffracted field components are shown in Fig. 4. Thus, the Green's functions $G^{direct}(x, y; x', y')$ and $G^{diff}(x, y; x', y')$ can be represented as

$$G^{direct}(x, y;, x', y') = \frac{1}{2j} H_0^{(2)} (k_0\sqrt{(x-x')^2+(y-y')^2}) \quad (11)$$

$$G^{diff}(x, y; x', y') = \frac{1}{4j} H_0^{(2)}(k_0 s_1')D_h \cdot (s_1' s_1/(s'+s_1), \phi_1, \phi_1' = 0^\circ) \frac{e^{-jk_0 s_1}}{\sqrt{s_1}} + \frac{1}{4j} H_0^{(2)}(k_0 (s_1''+h))D_h((s_1''+h)s_1/(s_1^n+h+s_1), \phi_1, \phi_1' = 0^\circ) \frac{e^{-jk_0 s_1}}{\sqrt{s_1}} + \frac{1}{2j} H_0^{(2)}(k_0 s_1^m)D_h(s_1^m s_1/(s_1^m+s_1), \phi_1, \phi_1' = 0^\circ) \frac{e^{-jk_0 s_1}}{\sqrt{s_1}} + G^{diff}_{higher\ order\ diff.\ terms}. \quad (12)$$

where D_h is the two-dimensional UTD hard diffraction coefficient[7],[8], from the first term through third term in $G^{diff}(x, y; x', y')$ are terms due to single diffractions. We define $G^{diff}_{higher\ order\ diff.\ terms}$ as the higher order diffraction terms, which represent all terms except for the terms due to single diffractions.

The enforcement of the continuity condition of the tangential magnetic field over the apertures leads to following integral equations,

$$\frac{2V}{\eta h} - j\frac{k_0}{\eta_0}\varepsilon_r \int_0^h M_z^p(y')\, G(x, y; 0, y')dy' = \frac{k_0}{4\eta_0}\int_0^h M_z^p(y')\, G^{ext}(x, y; 0, y')dy' + \frac{k_0}{4\eta_0}\sum_{l=1}^{L}\int_{C_l} M_z^{c,l}(x')G^{ext}(x, y; x', 0)dx' \quad (13)$$

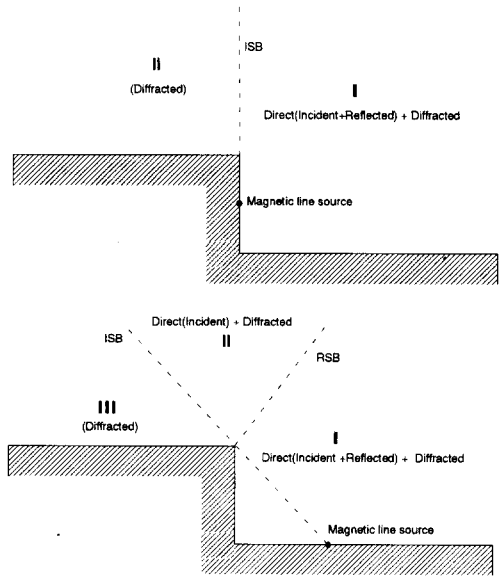

Fig. 3. Separation of the external region.

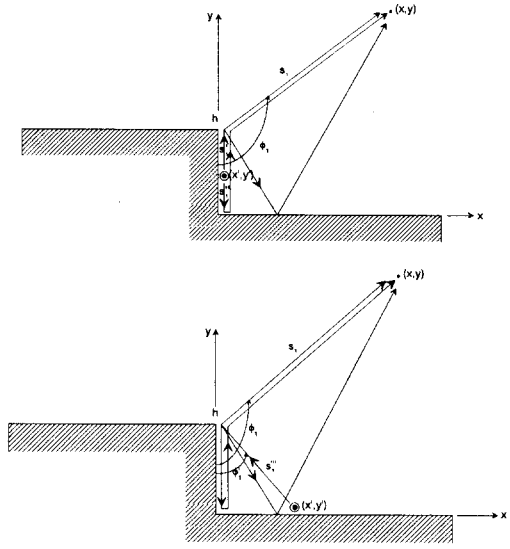

Fig. 4. Wedge diffracted field components.

$$-j\frac{k_0}{\eta_0}\varepsilon_{rc}\int_{C_l} M_z^{c,l}(x')\, G^{c,l}(x, y; x', 0)dx' = \frac{k_0}{4\eta_0}\int_0^h M_z^p(y')\, G^{ext}(x, y; 0, y')dy' + \frac{k_0}{4\eta_0}\sum_{l=0}^{L}\int_{C_l} M_z^{c,l}(x')\, G^{ext}(x, y; x', 0)dx' \quad (14)$$

where L is the total number of corrugations. The unknown currents M_z^p and $M_z^{c,l}$ can be expanded as a linear combination of pulses of the form

$$M_z^p(y') = \sum_{n=1}^{N_p} M_n^p P_n(y') \tag{15}$$

$$M_z^{c,l}(x') = \sum_{n=1}^{N_l} M_n^{c,l} P_n(x') \tag{16}$$

where P_n is the pulse basis function.

Applying the point-matching method on the above equation gives

$$\sum_{n=1}^{N_p} M_n^p \Big[j\frac{k_0}{\eta_0}\varepsilon_r \int_{y_n-\triangle/2}^{y_n+\triangle/2} G(x_m, y_m; 0, y')dy' + \frac{k_0}{4\eta_0}\int_{y_n-\triangle/2}^{y_n+\triangle/2} G^{ext}(x_m, y_m; 0, y')dy' \Big] + \sum_{l=1}^{L}\sum_{n=1}^{N_l} M_n^{c,l}\Big[\frac{k_0}{4\eta_0}\int_{x_n^l-\triangle_l/2}^{x_n^l+\triangle_l/2} \cdot G^{ext}(x_m, y_m; x', 0)dx' \Big] = \frac{2V}{\eta h} \tag{17}$$

$$\sum_{n=1}^{N_p} M_n^p \Big[\frac{k_0}{4\eta_0}\int_{x_n-\triangle/2}^{x_n+\triangle/2} G_{ext}(x_m^r, y_m^r; 0, y')dy' \Big] + \sum_{l=1}^{L}\sum_{n=1}^{N_l} M_n^{c,l}\Big[j\frac{k_0}{\eta_0}\varepsilon_{rc}\int_{x_n^l-\triangle_l/2}^{x_n^l+\triangle_l/2} \cdot G^{c,l}(x_m^r, y_m^r; x', 0)dx'\delta_{r,l} + \frac{k_0}{4\eta_0} \cdot \int_{x_n^l-\triangle_l/2}^{x_n^l+\triangle_l/2} G^{ext}(x_m^r, y_m^r; x', 0)dx' \Big] = 0 \tag{18}$$

where $\triangle$ is the pulse segment length of aperture of parallel-plate waveguide and $\triangle_l$ is the pulse segment length of l-th corrugaton slot. If we express the above equations as forms of admittance matrix, it can be shown as

$$\sum_{n=1}^{N_p} M_n^p \Big[j\frac{k_0}{\eta_0}\varepsilon_r Y_{mn}^{pp,il} + \frac{k_0}{4\eta_0} Y_{mn}^{pp,e} \Big] + \sum_{l=0}^{L}\sum_{n=1}^{N_l}\Big[\frac{k_0}{4\eta_0} Y_{mn}^{pl,e} \Big] = \frac{2V}{\eta h}, \tag{19}$$

$$\sum_{n=1}^{N_p} M_n^p \Big[\frac{k_0}{4\eta_0} Y_{mn}^{rp,e} \Big] + \sum_{l=1}^{L}\sum_{n=1}^{N_l} M_n^{c,l} \cdot \Big[j\frac{k_0}{\eta_0}\varepsilon_{rc} Y_{mn}^{rl,i2}\delta_{r,l} + \frac{k_0}{4\eta_0} Y_{mn}^{rl,e} \Big] = 0 \tag{20}$$

where

$$Y_{mn}^{pp,il} = \sum_{q=0}^{\infty} \frac{\varepsilon_q}{hjk_q} \cos\frac{q\pi}{h} y_m \cos\frac{q\pi}{h} y_n \cdot \frac{\sin(\frac{q\pi}{h}\frac{\triangle}{2})}{\frac{q\pi}{h}\frac{\triangle}{2}} \triangle \tag{21}$$

$$Y_{mn}^{rl,i2} = \sum_{q=0}^{\infty} \frac{-\alpha_q}{wk_q^c d\tan k_q^c d} \cos\frac{q\pi}{w} \cdot (x_m^r - x_c^l - \frac{w}{2})\cos\frac{q\pi}{w}(x_n^l - x_c^l - \frac{w}{2}) \cdot \frac{\sin(\frac{q\pi}{w}\frac{\triangle_l}{2})}{\frac{q\pi}{w}\frac{\triangle_l}{2}} \triangle_l \tag{22}$$

$$Y_{mn}^{uv,e} = Y_{mn}^{uv,direct} + Y_{mn}^{uv,diff}, \quad u \text{ and } v = p \text{ or } r \tag{23}$$

$$Y_{mn}^{uv,direct} = \begin{cases} 2\triangle(1 - j\frac{2}{\pi}\ln\frac{k_0 r\triangle}{4e}), & m=n,\ u=v=p, \\ 2\triangle_l(1 - j\frac{2}{\pi}\ln\frac{k_0 r\triangle_l}{4e}), & m=n,\ u=v=r=l, \\ 2\sum_{i=1}^{M} H_0^{(2)}(k_0\sqrt{(x_m^r - x_n^l - x_i)^2 + y_m^{r^2}})\frac{\triangle_l}{M}, & \left\langle \begin{matrix} m\neq n,\ u=p \text{ or } u=r,\ v=l \\ x_i = -\frac{\triangle_l}{2} + \frac{\triangle_l}{2M} + (i-1)\frac{\triangle_l}{M} \end{matrix} \right\rangle \\ 2\sum_{i=1}^{M} H_0^{(2)}(k_0\sqrt{x_m^{r^2} + (y_m^r - y_n^l - y_i)^2})\frac{\triangle}{M}, & \left\langle \begin{matrix} m\neq n, u=p \text{ or } u=r,\ v=p \\ y_i = -\frac{\triangle}{2} + \frac{\triangle}{2M} + (i-1)\frac{\triangle}{M} \end{matrix} \right\rangle \end{cases} \tag{24}$$

$$Y_{mn}^{uv,diff}=\begin{cases}\sum_{i=1}^{M} G^{diff}(x_m^r, y_m^r, x_n^l+x_i, 0)\frac{\triangle_l}{M}, \\ \quad u=p \text{ or } u=r,\ v=l \\ \sum_{i=1}^{M} G^{diff}(x_m^r, y_m^r, 0, y_n^l+y_i)\frac{\triangle}{M}, \\ \quad u=p \text{ or } u=r,\ v=p\end{cases} \tag{25}$$

and $\gamma=0.5772$, $e=2.718$ and M is the segmentation number which segment the pulse length $\triangle$ and $\triangle_l$.

In the form of the admittance matrix, the above equations are shown as

$$\begin{bmatrix} Y^{pp} & Y^{pc} \\ Y^{cp} & Y^{cc}\end{bmatrix}=\begin{bmatrix} V^p \\ V^c\end{bmatrix}\begin{bmatrix} I^p \\ 0\end{bmatrix} \tag{26}$$

Eq. (26) represents the linear equation. After solving this matrix equation and finding the unknown coefficients V^p and V^c indicating the equivalent magnetic currents M_z^p and $M_z^{c,l}$, one can readily compute all fields in each region.

Ⅲ. Numerical results and discussion

Before we design the end-fire corrugated surface wave antenna, we applied our method into the corrugated surface ("soft" surface) which is used for the corrugated horn antenna design. Fig. 5 shows the amplitude of the total magnetic field for the structure having $\varepsilon_r=\varepsilon_{rc}=1$, $h=0.4\lambda$, $w=0.1\lambda$, $T=0.125\lambda$, $d=0.25\lambda$ when the number of corrugation is 0, 5 and 10. It is observed from Fig. 5 that the end-fire radiation is reduced, and the maximum radiation angle is changed toward the broad-side when the corrugation number is increased. From Fig. 6 it is seen that the amplitude of magnetic currents at the apertures satisfies the edge condition of the magnetic currents, the magnetic currents toward end-fire is decreased as more corrugations are added.

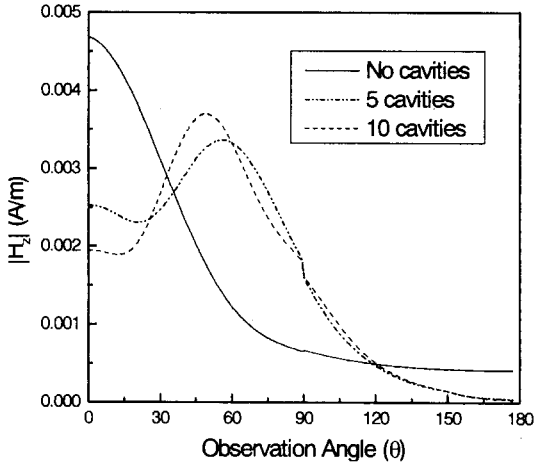

Fig. 5. Amplitude of magnetic field: $T=0.125\lambda$, $w=0.1\lambda$, $d=0.25\lambda$, $h=0.4\lambda$, $\varepsilon_r=1$, $\varepsilon_{rc}=1$.

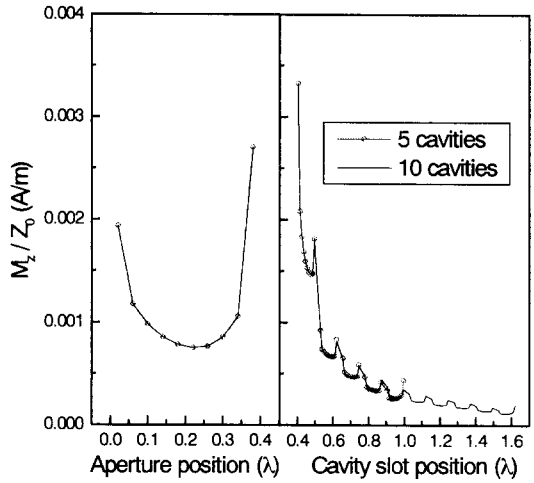

Fig. 6. Amplitude of surface magnetic current: $T=0.125\lambda$, $w=0.1\lambda$, $d=0.25\lambda$, $h=0.4\lambda$, $\varepsilon_r=1$, $\varepsilon_{rc}=1$.

To design the end-fire corrugated surface wave antenna, two relations[4] are used, which are Hansen-Woodyard and β/k_0-d relations. First, from $\tan k_0 d=\sqrt{(\beta/k_0)^2-1}$ (β/k_0-d relation), the corrugation depth is calculated, then the other parameters are determined by using $\beta/k_0=1+$

$\lambda/2L_{tot}$(Hansen-Woodyard relation), where L_{tot} is the total corrugated surface length. From these two relations, we obtain the parameters as follow $L_{tot}=7.33\lambda$, $\beta/k_0=1.07\lambda$ and $d=0.05798\lambda$. Our results are compared with those[4] solved by approximation method putting a more simplified equivalent current over the apertures of guide and corrugations. As seen from Fig. 7, they have, on the whole, similar shapes each other, but there are much differences in the beamwidth and sidelobe level. Also, our results are compared with the experiments[4] used a corrugated surface which was 2λ wide and 7.33λ long embedded in a ground plane 40λ wide and 70λ long, with the corrugation dimensions adjusted to give $\beta/k_0=1.07$, consistent with Hansen-Woodyard relation. Experiment patterns were taken using a receiving horn which was mounted on a rotatable arm 50λ long, thereby simulating the far-field measurements for the case of an infinite ground plane. With $h/\lambda=0.73$, the experimental pattern which was obtained at 9.840 GHz is shown as the line with circle symbol in Fig. 7. Our results are much well matched with those of the experiment except the slight difference in the sidelobe levels. The beamwidth and deep points(null angles) are almost same. Therefore, we can conclude that our method provides more accurate results. From Fig. 8, it is seen that the amplitude of magnetic currents at the corrugation surface is changing sinusoidally, that is, a surafce wave is guiding toward end-fire direction.

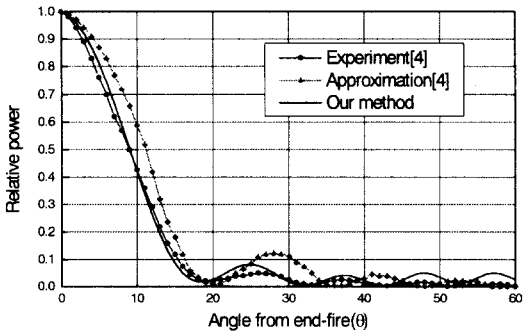

Fig. 7. Relative power pattern for a corrugated surface antenna: $T=0.125\lambda$, $w=0.1\lambda$, $h=0.73\lambda$, $\varepsilon_r=1$, $\varepsilon_{rc}=1$, $L=58$, $L_{tot}=7.33\lambda$, $\beta/k_0=1.07\lambda$, $d=0.05798\lambda$.

Fig. 9 shows the relative power for different values of β/k_0 consistent with Hansen-Woodyard relation when h is 0.4λ. The smaller β/k_0 is, the higher the sidelobe level is, but the beamwidth is narrower. Fig. 10 shows the relative power for different values of h. The smaller h is, the higher the sidelobe level is, however, but the beamwidth is wider slightly. Thus, to meet the moderate sidelobe level and beamwidth, a tradeoff is needed.

Our method is very efficient to analyze the proposed surface wave antenna by introducing the UTD to get approximate Green's function of the external region because it is difficult to obtain exact Green's function of the external region

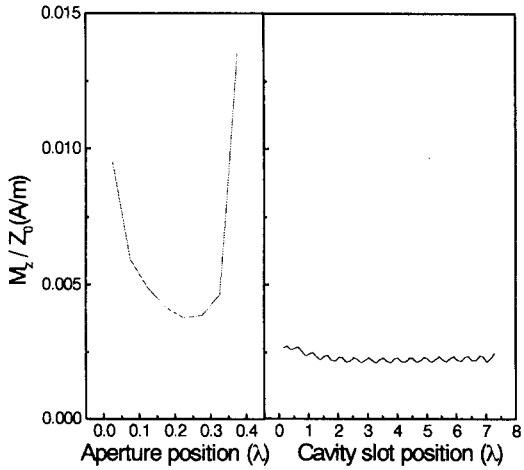

Fig. 8. Amplitude of surface magnetic current : $T=0.125\lambda$, $w=0.1\lambda$, $h=0.73\lambda$, $\varepsilon_r=1$, $\varepsilon_{rc}=1$, $L=58$, $L_{tot}=7.33\lambda$, $\beta/k_0=1.07\lambda$, $d=0.05798\lambda$.

by the complexity of the geometry. The numerical efficiency of the hybrid MOM/UTD is related to how many higher order diffracted terms are accounted to calculate the external Green's function more exactly. However, the higher order diffracted terms expressed in the Green's function are simple functions, thus those have almost no effect on the numerical evaluation.

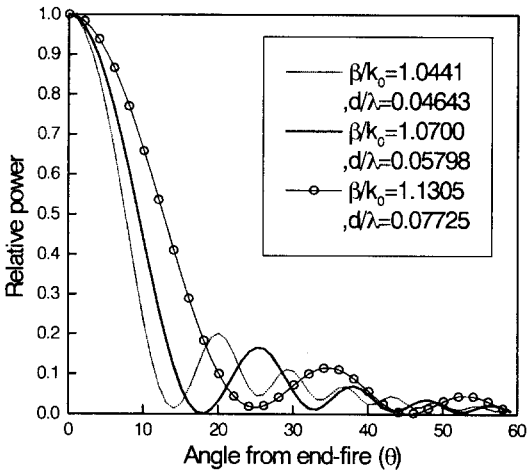

Fig. 9. Relative power patterns for different values of β/k_0 : $T=0.125\lambda$, $w=0.1\lambda$, $h=0.4\lambda$, $\varepsilon_r=1$, $\varepsilon_{rc}=1$.

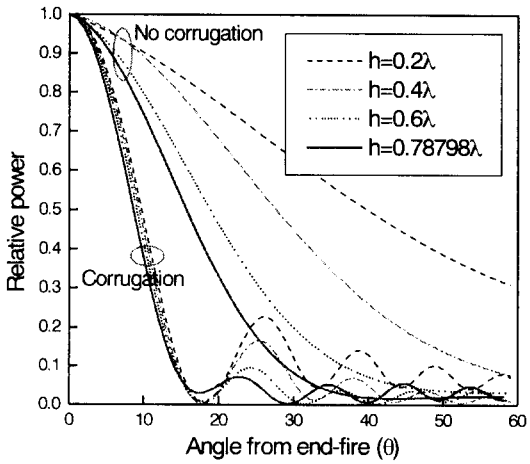

Fig. 10. Relative power patterns for different values of h : $T=0.125\lambda$, $w=0.1\lambda$, $\varepsilon_r=1$, $\varepsilon_{rc}=1$, $L=58$, $L_{tot}=7.33\lambda$, $\beta/k_0=1.07\lambda$, d=0.05798λ.

Ⅳ. Conclusion

A hybrid MOM/UTD method was presented for the analysis of the surface wave antenna with the corrugated surface in an infinite ground plane fed by the parallel-plate waveguide. The presented approach employed the equivalent theorem to lead to a simplification of the analysis. Thus, the problem domain was subdivided into one external region and two internal regions. The external region consists of the conducting wedge with the equivalent currents as additional sources. The Green's function of the external region was found via UTD, i.e., the sum of the geometrical optics and the wedge diffracted terms. The Internal region 1 and 2 consist of inside the shorted parallel-plate and the cavities of the corrugation, respectively. The Green's functions of the interior region were analytically obtained in terms of the modal function. By applying the boundary condition and MOM, the fields in each region were obtained. The relative power pattern of the present method was compared with that of the previous approximation solution and the experiment. Our results are much well matched with those of the experiment. Therefore, the present method is very useful for obtaining the accurate result. We also investigated the effects of the parameters needed to design a practical end-fire corrugated surface wave antenna. The present method is applicable to the corrugated horn antenna design. Future extensions of this work include the corrugated surface antenna with finite ground plane.

References

[1] C. H. Walter, *Travelling Wave Antennas.* New York : McGraw-Hill Book Co., Inc., 1965, pp. 258-268

[2] R. E. Collin and Francis J. Zucker, *Antenna Theory Part 2.* New York : McGraw-Hill, 1969.

[3] H. Jasik, *Antenna Engineering Handbook.* New York: McGraw-Hill, 1961.

[4] R. S. Elliott, *Antenna Theory and Design.* Englewood Cliffs, New Jersey : Prentice-Hall Inc., 1981, pp. 429-453

[5] R. F. Harrington and J. R. Mautz, "Generalized network formulation for aperture problems," *IEEE Trans. Antennas Propagat.*, AP-24, pp. 870-873, Nov. 1976.

[6] A. Borgioli, R. Coccioli and G. Pelosi, "Electromagnetic Scattering from a corrugated wedge," *IEEE Trans. Antennas Propagat.*, AP-45, pp. 1265-1269, August 1997.

[7] R. G. Kouyoumjian and P. H. Pathak, "A uniform geometrical theory of diffraction for an edge in a perfectly conducting surface," *Proc. IEEE*, vol. 62, pp. 1448-1461, Nov. 1974.

[8] D. A. McNamara, C. W. I. Pistorius and J. A. G. Malherbe, *Introduction to The Geometrical Theory of Diffraction.* Boston, London: Artech House, 1990, ch. 4,5.

김 중 표

1991년 2월: 경북대학교 전자공학과 (공학사)
1993년 2월: 경북대학교 대학원 전자공학과(공학석사)
1993년 3월~현재: 경북대학교 대학원 전자공학과(박사수료)
[주 관심분야] 전자파 산란 및 안테나 해석

이 창 원

1991년 2월: 경북대학교 전자공학과 (공학사)
1993년 2월: 경북대학교 대학원 전자공학과(공학석사)
1998년 8월: 경북대학교 대학원 전자공학과(공학박사)
[주 관심분야] 전자파 산란 및 안테나 해석

손 현

1960년 8월: 연세대학교 전기공학과 (공학사)
1975년 8월: 한양대학교 대학원 통신공학과(공학석사)
1984년 8월: 경희대학교 대학원 전자공학과(공학박사)
1966년 4월~1977년 4월: 주한 미육군 정보통신단 작전과 기술지원실 기술부장
1977년 4월~현재: 경북대학교 전자공학과 교수
[주 관심분야] 이동통신, 위성통신, 마이크로파 및 안테나